7-45-41

# ATMOSPHERIC SPRAY-CANAL COOLING SYSTEMS FOR LARGE ELECTRIC POWER PLANTS

R.W. Porter and S.K. Chaturvedi
Illinois Institute of Technology
Chicago, Illinois U.S.A.

## ABSTRACT

Spray cooling systems are alternatives to cooling ponds and evaporative cooling towers for power plant condensers and nuclear ultimate heat sinks. Mathematical modeling is reviewed and simplified solutions are presented for thermal performance as a heat exchanger. The Number of Transfer Units (NTU) and a dimensionless air-vapor interference allowance were determined experimentally for "Ceramic" and "Richards" spray modules at Commonwealth Edison Company's Quad-Cities and Dresden Nuclear Stations in Illinois wherein spray canals are used for condenser cooling. The simplified NTU analysis provides an adequate basis for correlation of performance in terms of spray drop-wise parameters. The critical factor appears to be the interference allowance as governed by air-vapor flow and atmospheric dispersion.

## INTRODUCTION

### Summary

It is essential that reliable prediction techniques be available to insure proper cooling capacity for condenser heat rejection to the atmosphere from large electric power plants. Under design will result in decrease in thermal efficiency and, in the extreme, de-rating of generating capacity. Over design adversely affects energy costs and may even lead to exclusion from further consideration of an otherwise favorable system. The problem is acute for new larger plants of immense capital investment but which best utilize national energy resources, especially those of nuclear power and coal.

Cooling systems are also essential for various plant auxiliaries and the so-called ultimate heat sinks (UHS) of nuclear-reactor safety logistics. In this case, dissipation



RWP

of heat according to a prescribed history over an extended period is critical, and a validated design technique is mandatory.

Open spray cooling systems are an alternative to cooling ponds and evaporative cooling towers for supplemental or closed-cycle applications. Factors of land availability, cost and environmental impact must be considered on an individual basis. The spray canal wherein floating spray modules are placed mainly in series in an open channel has evolved for the condenser application. The channel typically contains $10^6$ gpm ($4 \times 10^6$ liters/min) of water with each module delivering about $10^4$ gpm ($4 \times 10^4$ l/m) of about 1-cm diameter drops, power by a nominally 75-hp (56-Kw) motorized pump. The spray pattern is about 5 m high and extends over from 200-600 $m^2$ of canal surface depending on the particular design. Both manifolded multiple cone-impact and single circular-slot nozzle designs have been utilized. The large drop size and relatively massive spray are compatible with the desire for large flow rates and small drift loss with the prevailing wind substantially in cross flow to the canal. Conversely, the finer in-place manifolded spray matrix has evolved for the spray-pond application to the UHS. In this case order-mm-diameter drops are generated in smaller sprays. The drop-wise parameters of the spray may be combined into a dimensionless group, Number of Transfer Units (NTU), which may be used to predict spray cooling range in terms of initial liquid temperature T and local wet-bulb temperature (WBT). The latter may be related to ambient WBT and T through a dimensionless interference allowance f which includes localized heating and humidification effects as well as larger-scale convective diffusion in the atmospheric boundary layer with an imbeded spray matrix.

The present paper summarizes the results to date of the IIT Waste Energy Management Project in the area of field experiments for determination of NTU and interference-allowance f carried out at Commonwealth Edison Company's Dresden and Quad-Cities Nuclear Stations which employ spray canals. A complete tabulation of the experimental results is contained in [1]. While experimental data are presented for local air-vapor interference which results in greater-than-ambient local wet-bulb temperature, comprehensive modeling of this aspect is reported in [2]. Dispersion of the buoyant discharge downwind is to appear separately. A complete evaluation of equations for direct-contact evaporative



RWP

cooling for open sprays including solar and atmospheric radiation and non-unit psychrometric ratio which are neglected in the Merkel's equation most often applied is contained in [3]. The present data were correlated with the more detailed theory for selected cases in [1]. However, the simplified analysis [4] summarized here is adequate so long as the correct local interference allowance is used.

The field experiments reported earlier [3] for Dresden Station (Morris,Illinois) involved measuring canal temperatures upstream and downstream of a run of up to 40 4-spray Ceramic Cooling Tower Company (CCT) modules [5,6] arranged 2 units (modules) wide across the canal (Figure 1). Module parameters are summarized in Table 1. Correlation allowed for time of flow and average meteorological conditions. These data were used to imply canal-averaged NTU based on a previously assumed dimensionless interference allowance f to account for local elevation of wet-bulb temperature. A spray collection device was subsequently used to determine local NTU in various portions of the upwind and downwind sprays. The module NTU measurements were also accomplished at the 4-units-wide spray canal at Quad-Cities Nuclear Station (Cordova, Illinois) wherein are employed 176 CCT modules (Figure 2) and 152 single-spray Richards of Rockford (RR) modules [5,7] (Figure 3). However, at Quad-Cities additional measurements were made of actual local wet-bulb temperature and wind speeds as a function of the row position proceeding downwind. Thus, both local NTU and local dimensionless interference allowance were determined. The NTU data are correlated best with wind speed although wind angle, bank height and a natural convection parameter were also considered. By turning off one spray module at a time, it was possible to imply the difference between total and self interference; that is, of the entire system and of the individual module, respectively. Self interference is quite appreciable, and the first upwind row does not see the ambient WBT nor does absorbing self interference in NTU adequately scale the increment thereof for a single spray. Accounting for interference, NTU from canal (Dresden) and module (Dresden and Quad-Cities) experiments are in essential agreement. It now appears that NTU is the more easily established quantity and does not vary greatly over various operating conditions for a particular module(usually less than ±15%). On the other hand, dimensionless interference allowance requires more comprehensive modeling [2].



RWP

Review of Literature

Heat and mass transfer of liquid-water spray cooling in air and water vapor mixtures may be classified according to: 1. fundamental aspects, 2. droplet phenomena, 3. air-vapor flow, 4. unit and system performance. It is possible to go directly from Item 1 to 4 if the unknown parameters are determined experimentally. This approach is used in the present study although the other categories are briefly summarized.

Fundamental aspects of simultaneous heat and mass transfer are reviewed in detail in [8,9] as well as in many other standard texts. Both heat and mass transfer are governed by convective diffusion equations but the diffusivities a and D, respectively, differ in general. The interface between liquid and gas phases is bounded by saturated liquid and saturated vapor in air. The most general approach utilizes separate correlation for the sensible heat transfer coefficient H, and the mass transfer coefficient K. The total energy transport is due to the former involving temperature difference, and the latter which is due to vapor mass fraction difference. For air and water vapor, typically 85% of the energy transport is due to evaporation carrying enthalpy with it.

In practice, simultaneous correlations for heat and mass transfer are seldom available for geometries and dimensionless group ranges of interest. However, consideration of a wide range of theory and experiments has led to the "analogy of heat and mass transfer" wherein H and K are related by the psychrometric ratio P. For temperatures of interest, 0-50 C, and atmospheric pressure, Threlkeld reviewed the available data and concluded [9]

$$P = H/(c_s K) \approx (a/D)^{2/3} \qquad (1\text{-}1)$$

where $c_s$ is humid heat, the specific heat of air and vapor at constant pressure per unit mass of (dry) air. Because $a/D \approx 1$ for air and water vapor, $P \approx 1$ which leads to considerable simplification and the well-known Merkel equation for direct-contact evaporative cooling. In this case, the net driving potential for energy transport is Carrier's sigma function or total heat, a specific enthalpy referenced to the saturated liquid state which depends only on WBT.



RWP

Droplet phenomena refers to the "near field" about individual droplets. The break-up of liquid jets into droplets depends on the balance between surface tension, internal circulation and aerodynamic forces including turbulent fluctuations [10]. The atmospheric free-fall velocity from a typical 5-m spray height is about 10 m/s which corresponds to a terminal velocity for about 7-mm diameter drops [11]. Larger drops than this are subject to very near the parabolic trajectory of free flight.

In principle, it is possible to solve simultaneously the fluid mechanics both within and outside a droplet if approximations are made in terms of spherical shape, high Reynolds number and uniform drop environment [12,13]. However, the departure of liquid drops from solid spheres in terms of heat and mass transfer is generally recognized, the classical correlations for steady state being due to Ranz and Marshall [14]. Recent studies by Yao and Schrock [15] are devoted toward correcting these correlations for freely falling drops. Given the drop-size distribution such as determined experimentally by optical techniques [16], it is nevertheless feasible to compute theoretical temperature-time histories and integrate these into bulk flow averages [17]. Hollands and Goel [18] relate NTU to such distributed effects through the definition of a mean particle (drop) size.

The problem of air-vapor flow through sprays was analyzed by Porter and Coworkers[3-5] through the experimentally determined dimensionless interference allowance which scales wet-bulb temperature increment with the difference between water temperature and ambient WBT. In [3] it is related to the effective L/G (liquid to gas) ratio of the flows. However, because air-vapor flow is not subject to well-defined channeling as in a cooling tower, the L/G parameter can not be realistically predicted. An alternate approach, due to Elgawhary and Rowe [19], defines an air cell which follows the droplets and receives the heat and mass transfer. The radius of the air cell is determined experimentally. Other similar models are reviewed by Ryan and Myers [20].

The most valid approach from a physical point of view is due to Chen and Trezek [21]. A quasi one-dimensional momentum balance on the spray is used to compute exit vertical and horizontal velocity in a step by step procedure

going downwind. The forces are computed from theoretical drop drag forces integrated over an experimental drop-size distribution. In between sprays, an assumed ambient flow over the sprays is mixed with the horizontal exit flow using Schlicting's planar turbulent jet mixing solution [22]. However, Chen and Trezek must increase mixing by a factor of 135 to agree with their experiments using five sprays aligned with the prevailing wind. A major part of the discrepancy may be due to planar jet mixing not being the controlling phenomena,and three-dimensional end effects.

Unit and system performance relates to the cooling achieved by an individual spray or spray module (i.e., a unit) and an assembly of units (the system). Ryan and Meyer [20] summarize the various techniques in general. The discussion here will be limited to essentially NTU (Number of Transfer Unit) methods wherein the drop-wise parameters are combined into a dimensionless group (NTU or equivalent). Quantity NTU may be predicted from droplet theory or implied from measured cooling ranges of experiments. Other methods include detailed analysis of drop time-temperature histories without reduction to NTU or are fully empirical.

The NTU method for open sprays appears to originate with Kelley [7,23]. An average "enthalpy" difference was used in the NTU equation,and a step-by-step marching procedure was employed for canal performance. Hoffman [24] reported system performance data for several spray canals in terms of observed cooling range. Porter and Chen [5] reduced this data to NTU correcting for local WBT elevation using the nondimensional interference allowance f as determined from measurements at Dresden station downwind of sprays. Superposition was used to account for multiple upwind rows, and local "self" interference was neglected.

Porter [4] also developed a simplified analytical solution by assuming total heat is linear with adiabatic-saturation temperature and correlated the Hoffman data [24]. Later this method and a linearized corrected one including psychrometic ratio,radiation,etc.,were applied to new experimental data directly taken by Porter and Coworkers at Dresden Station [3]. The corrections were found to be small. More important, values of NTU were found to be substantially lower than previously reported. This data is substantiated here as compared with the recent measurements on individual modules at both Dresden and Quad-Cities Stations.



RWP

Chen and Trezek [21] developed an NTU method for spray ponds but define NTU as "SER" (Spray Energy Release). The main feature of the SER method ,already discussed, is that the energy release of the spray is used to compute that gained by the air and vapor. Soo has shown the equivalence of the several approaches to the NTU method [25] and as an application considers the optimized performance of a spray-module system in terms of drop size and spray height as they affect pumping power for cooling duty. He concludes [26] optimum drop size is about 5-mm diameter and spray height about 4 m based on approximations and criteria employed.

Arndt and Barry [27] have developed a computer program that treats each spray element as a point source. Heat and humidity release is analyzed using NTU [24], and dispersion rates from air-pollution studies are used to determine local wet-bulb temperature by superposition and iteration. The recent approach of the present investigators [2] includes wind attenuation and atmospheric dispersion coupled with variable heat and humidity release in a unified fluid-dynamic analysis. Effects of parameters on systems performance are also discussed.

## THEORETICAL ANALYSIS

### Unit Performance

The statements of conservation of energy and mass for a steady monodisperse(single drop size) liquid-spray flow with an exposed surface-area element dA, as in control Volume I of Figure 4 are

$$d\left(\dot{m}_s i_L(T')\right) - i_g(T')\,d\dot{m}_s = H\,dA(T_{DB}-T') \qquad (2\text{-}1)$$

$$d\dot{m}_s = K'dA\left[\omega/(1+\omega) - \omega_S(T')/(1+\omega_S(T'))\right] = K'/(1+\bar{\omega})\cdot dA(\omega-\omega_S(T')) \qquad (2\text{-}2)$$

where $\dot{m}_s$ is spray mass flow rate, i water specific enthalpy, H sensible heat transfer coefficient, T temperature, K mass transfer coefficient based on (water) vapor mass fraction, a fundamental driving potential for mass transfer [28], $\omega$ is specific humidity (mass of vapor per mass of dry air), and s denotes spray, L liquid water, g saturated water

vapor, DB dry-bulb temperature (DBT), S saturated air-vapor mixture, prime the local spray temperature, and the bar an average condition. By definition, H and K are based on contact area A. Effects of the drop-size distribution are discussed at the end of the present section. Radiation is included in the corrected analysis of [1,3] but is neglected here.

Assuming $i_L = i_f$ where f denotes saturated liquid and $di_f = c_w dT'$ where $c_w$ is specific heat of liquid water, assumptions which are virtually exact for present purposes, the above combines to

$$\dot{m}_s c_w dT' = -K\, dA \left(Pc_s(T' - T_{DB}) + i_{fg}(T')(\omega_S(T') - \omega)\right) \quad (2\text{-}3)$$

where $P = H/(c_p K') = H/(c_s K)$ is the psychrometric ratio, $i_{fg}$ is water latent heat, $c_p$ is specific heat, $c_s = (1+\bar{\omega})c_p$ is the humid heat and $K = K'/(1+\bar{\omega})$. Note that the factor $1+\bar{\omega}$ has been absorbed, and no appreciable error has been introduced by using humidity as the driving potential.

It is convenient to recast Eq.(2-3) in terms the air-vapor wet-bulb temperature (WBT) $T_{WB}$ which is the equilibrium liquid water temperature T', when Eq.(2-3) is identically zero. Substituting this expression to eliminate $T_{DB}$ and $\omega$, the result is

$$\dot{m}_s c_w dT' = -K\, dA \left[h(T') - h(T_{WB}) - c_{pa}(1 - Pc_s/c_{pa})(T' - T_{WB}) - \omega(i_{fg}(T') - i_{fg}(T_{WB}))\right] \quad (2\text{-}4)$$

where h is Carrier's sigma function (total heat) which is defined as [29]

$$h(T_{AS}) \equiv \hat{i}(T_{DB}, ) - \omega i_f(T_{AS}) \approx c_{pa}\, T_{AS} + \omega_S(T_{AS})\, i_{fg}(T_{AS}) \quad (2\text{-}5)$$

Quantity $T_{AS}$ denotes adiabatic-saturation temperature (AST), i is enthalpy of air and vapor per unit mass of dry air and $c_{pa}$ is specific heat of dry air. Quantity h is tabulated in [29]. The AST is a thermodynamic property while the WBT is a transport property which is the same for the spray and a wetted-wick psychrometer presuming equal psychrometric ratios P. The relationship between AST and WBT is given in [1,3,9]. For air and water vapor where $P \approx 1$, the



RWP

difference between them is of order 0.1 C and is of secondary importance [1,3].

Assuming $Pc_s/c_{pa} = 1$ and neglecting the variation in latent heat, assumptions relaxed in [1,3] and also shown to be of secondary importance

$$c_w \int_{T_s}^{T} \frac{dT'}{h(T')-h(T_{WB})} = NTU \qquad (2\text{-}6)$$

where the Number of Transfer Units $NTU \equiv \overline{KA/\dot{m}_s}$, T is the canal temperature at the spray nozzle intake and $T_s$ is the final sprayed water temperature. Eq.(2-6) is Merkel's equation of direct-contact evaporative cooling. In a cooling tower, a similar energy balance on the air and vapor yields $dh(T_{WB})/dT = -c_w L/G$ where L/G is the liquid-to-gas mass ratio [30]. In the present case L/G is not well defined and so an average local $T_{WB}$ is used instead. The relation of $T_{WB}$ to the ambient $T_{WB\infty}$ is through the "interference allowance" discussed later.

In the present simplified analysis, Eq.(2-6) is integrated by assuming $b = dh(T)/dT = b(T_f) \equiv b_f$, a constant, where $T_f$ is a "film temperature" used for property evaluation. Quantity b is tabulated in Table II using h(T) data of [29]. For a temperature interval bounded by $T_{WB\infty}$ and $T_H$, a hot water temperature, it is suggested to use $T_f = (T_H + T_{WB\infty})/2$. Because the quantity b is slowly varying, no appreciable error is introduced in typical cases as shown in [1,3]. Thus, the dimensionless module cooling range is

$$(T-T_s)/(T-T_{WB}) = 1-\exp(-ntu\ b_f/c_w) \qquad (2\text{-}7)$$

where a new symbol ntu is used for NTU in order to distinguish the specific theory utilized when Eq.(2-7) is used to imply NTU from experimentally observed temperatures. For example, in [1,3] it is shown that experimentally implied NTU do differ slightly when non-unit psychrometric ratio, radiation and nonlinear total heat are incorporated in more general theory. The designation NTU is used in a broad sense to indicate $\overline{KA/\dot{m}_s}$.

In [4,5], NTU is defined in terms of an average-drop



RWP

trajectory analysis where it is shown NTU = $(\overline{K_d A_d/m_d})t$ where m is mass, t time of flight and d denotes drop. The droplet approach has also been used by Chen and Trezek [21] and Soo [25,26]. It is apparent that NTU for the overall spray interface and the mean drop trajectory are equivalent and equal when they lead to the same equation (2-7).

As discussed at the onset, the basic equations (2-1) and (2-2) apply to a monodisperse system. Drop-size distribution will result in variable exchange with the environment causing a drop-size dependent distribution of temperature and evaporation as modified by heat and mass interchange due to drop break up and coalescence. Quantity NTU may be regarded as that of an equivalent monodisperse system of appropriate mean drop size if certain conditions are met, namely combined heat and mass transfer with a Merkel-type equation, uncoupled drop motion, and negligible drop internal thermal resistance [18]. In particular, the last condition may not be entirely realistic [15]. Thus, for sprays of appreciable drop size distribution, the apparent NTU may depend to some extent on prevailing conditions. The most direct measurement of NTU involves sampling the spray temperature of individual modules and determining the local average WBT. Eq.(2-7) then yields NTU or more precisely ntu, to identify the theory used. Results are discussed in the next major section.

The evaporation can be computed by integrating Eq.(2-2) or by using an average Bowen ratio of sensible to evaporative heat transfer $\bar{B} = (Pc_s/\lambda_{fg})(\bar{T}-T_{DB})/(\omega_s(\bar{T})-\omega)$ where $\bar{T}$ is an average liquid water temperature and $Pc_s/\lambda_{fg} \approx 0.00038\ C^{-1}$. In this case the fraction of spray flow rate evaporated is directly related to the spray cooling.

$$\alpha = (c_w/\lambda_{fg})(T-T_s)/(1+\bar{B}) \qquad (2\text{-}8)$$

where $c_w/\lambda_{fg} \approx 0.0017\ C^{-1}$. Evaporation of sprayed water is small (typically 1 or 2%), and from the thermal point of view results are weakly dependent on $\bar{B}$. Thus, spray performance depends mainly on the wet-bulb temperature rather than both the dry-bulb temperature and the humidity. The upper limit on evaporative make-up water required can be computed assuming $\bar{B} = 0$.



RWP

Air-Vapor Circulation Interference

The air-vapor mixture is heated and humidified as it comes in contact with the spray. As noted earlier, for flow within a cooling tower this is accounted for by an energy balance $dh(T_{WB})/dT = -c_w L/G$. Integrating using $b_f = dh/dT_{WB}$ limits of $T_{WB_\infty}, T_{WB}$ and $T_s^w, T$ for L and G in counter flow, and (2-7)

$$T_{WB_1} = T_{WB_\infty} + f_1 (T - T_{WB_\infty}) \tag{2-9}$$

where for each row 1 of modules across the canal

$$f_1 = (c_w/b_f)(L/G)_1 (1 - \exp(-ntu\ b_f/c_w)) \tag{2-10}$$

It should be noted that the standard counter-flow configuration assumed is arbitrary. Further, values of L/G are virtually impossible to predict or measure for open sprays especially when imbeded in a spray system. Thus, Eq.(2-10) is not actually utilized by the present investigators except to demonstrate the basic nondimensional scaling in Eq.(2-9). A fluid dynamic theory for f based on analyzing wind attenuation and atmospheric diffusion is contained in [2].

The f quantity is bounded $0 \leq f \leq 1$ considering the possible interval between the ambient state and equilibrium with the canal. Like NTU, it contains parameters which may be predicted from more detailed theory, but which also may be implied experimentally in connection with Eq.(2-9) as discussed later.

Spray-Canal Peformance

As discussed in [3-5] typical spray canals are very well mixed, and so the temperature T is considered constant in a canal section. Across each pass of modules, n, the canal will be cooled according to the fraction of the canal water sprayed. For each row 1 of m rows across the canal, simple mixing considerations for Control Volume II (Figure 4) yield

$$dT_i/dn = -mr(T - T_{s1}) \tag{2-11}$$

where r is the ratio of module flow rate to initial canal flow rate and where the small loss of evaporative flow is neglected in the mass balance as justified in [1,3]. The

module cooling range $T-T_{s_i}$ is given by Eq.(2-7). Using Eqs.(2-7) and (2-9) in (2-11) and averaging across the canal to obtain the average dT/dn and integrating from the canal-intake hot water temperature (HWT)$T_H$ to the canal-discharge cold water temperature (CWT)$T_c$

$$(T_c-T_{WB_\infty})/(T_H-T_{WB_\infty}) = \exp\left[-Nr(1-\bar{f})\left(1-\exp(-ntu\ b_f/c_w)\right)\right] \quad (2\text{-}12)$$

where N = nm, the number of modules, and where $\bar{f}$ is the arithmetic average value for m rows across the canal.

While evaporation is small, it is important for make up including blow down and for environmental considerations. The rate of evaporation as a fraction of initial canal flow, e, is by definition given by $de/dn = mr\alpha$. This may be integrated from e(0) = 0 by using (2-8) and (2-11). The resulting exponential relation may be approximated

$$e = \left[c_w/\left(\lambda_{fg}(1+\bar{B})\right)\right](T_H-T_c) \quad (2\text{-}13)$$

and which also follows directly from the definition of Bowen's ratio. As an example, a 14-C cooling range leads to 2.4% evaporation of canal flow in the worst case of $\bar{B} = 0$.

The above approach assumes a steady state in terms of a uniform $T_{WB}$, ntu and f (meteorological dependent) as well as r and $T_H$ (canal-intake dependent). By using time-averaged-over-flow meteorological data, a "slug of fluid" can be followed through the canal by knowing the time of discharge into the system and the time of flow. Conversely, by measuring the temperatures, ntu can be implied. However, the circulation allowance $\bar{f}$ must be defined.

## FIELD EXPERIMENTS

### Instrumentation and Techniques

As summarized in Table III, both local module experiments and overall canal experiments were performed. In the former case, local WBT and wind speed and/or spray temperature were sensed. In the latter case, only canal temperatures at the ends of the run of modules were obtained.



RWP

Determination of ambient conditions was similar in both cases.

Canal and spray water temperatures were detected by Atkins thermistor sounding probes and bridges. In Exp. 1, canal water temperatures were monitored at a mid-channel location at the canal-segment intake and discharge ends. In module-NTU measurements (Exps. 2-5), canal water temperature was monitored locally at the test module or immediately upstream. A water collection device was designed and constructed to collect spray water after flight and measure a radially integrated spray temperature. The collector was a 3-ft diameter funnel and floated about 6 inches out of the water when operating. A thermistor was positioned at the throat in a shielded perforated case in about 4 inches of water. Measurements were made approximately every $90^{o}$ about the spray pattern proceeding from upwind rows. When the collector was properly positioned via cables from shore, the thermistor bridge was switched from the canal temperature sensor to the spray-collector temperature sensor and held for several minutes to get a gust-averaged value. Canal water temperature was monitored below the surface. As noted previously, experience has shown very little variation in canal temperature at a section.

Wet-bulb and dry-bulb temperatures were obtained from Atkins psychrometer modules and thermistor bridges. Wind run was determined from contact anemometers calibrated in the IIT 4 x 6 foot environmental wind tunnel to ±0.1 m/s. Wind direction was obtained with a bivane with a potentiometer element. Ambient meteorological conditions were measured sufficiently upwind to avoid interference and at a 2-m elevation over grade. Local conditions were measured directly over the module motor 2m over the water level. Bridges and recorders were calibrated in the field using a calibrated decade-resistance substitution device. Recorded temperature data were accurate within ±0.1C.

In canal-NTU tests, all meteorological data were subsequently averaged over the time of flow of each slug corresponding to a hot-water temperature (HWT) reading. The cold-water temperature (CWT) was read from the continuous data allowing for time of flow. Canal flow was determined using a Weathermeasure helical propeller contact flow meter and a Heath digital electronic depth sounder (±0.3m). The



RWP

canal bottom and banks were defined in contour and velocity-sounded at 3 equally spaced points each in width and depth. Velocity was first averaged in width and then the vertical profile was integrated graphically allowing for a thin viscous sublayer at the bottom. Resultant canal flow rates agreed with manufacturer's lift-pump specifications to ±5%.

In the module-NTU tests, spray temperature and local wet-bulb temperature were sampled sufficiently long to allow averaging over gusts. Typically, several (3-4) cycles were obtained over a few minutes duration. Canal temperature and ambient conditions were then referred to the test interval. In obtaining average wind speed, wind run was summed over the period. In most cases, it was not possible simultaneously to measure local wet-bulb temperature and spray temperature. This was due to the time-consuming procedure of moving the psychrometer from module to module in the various rows. In the Richards modules, the mooring cables were in the way of the collector which further slowed the process. Where simultaneous wet-bulb temperature was not available to correlate with spray temperature, the nearest-time data for dimensionless interference allowance was applied to the prevailing ambient wet-bulb and canal temperatures. This allowance corresponded to measurements under very similar conditions.

Time averaged parameters are listed in Table III. The natural-convection buoyancy parameter is the maximum possible fractional density increment of the air-vapor mixture as it is heated and humidified by spray at an average temperature $\bar{T}$. Thus

$$|\Delta\rho|/\rho = T_{DB_\infty}^{-1}(\bar{T}-T_{DB_\infty}) + (\omega_S(\bar{T})-\omega_\infty) \qquad (3\text{-}1)$$

where the first coefficient is approximately $-\rho^{-1}\partial\rho/\partial T$, $T_{DB\infty}$ is ambient absolute temperature and the second coefficient is $-\rho^{-1}\partial\rho/\partial\omega \approx 11/18$. Also listed are film temperature which gives the approximate temperature level of the overall system, wind speed (WS) wind direction (WD) in terms of angle of incidence to the canal, and bank height. A complete tabulation of individual temperature and other data is contained in [1]. The complete data for Exp. 1 is also tabulated in [3].



RWP

Local-Interference Data

The experiments wherein local WBT and wind-speed data were obtained are Exps. (3a)-(5b) of Table III. All data were obtained at the Quad-Cities Station 4-row canal. The location of the measurements for the Ceramic modules is noted by the solid squares in Figure 2. In the Richards case, measurements were on center of the circles (sprays) of Figure 3. The basic approach was to alternately take measurements with the module tested both on (spray on) and off (spray off) while the other modules were running. The difference in readings is attributed to "self interference". Some data were also taken with a single module or single row of modules (denoted S). The psychrometer and anemometer were not submerged in the spray itself.

As discussed previously, the appropriate nondimensional WBT interference allowance is defined

$$f \equiv (T_{WB}-T_{WB_\infty})/(T-T_{WB_\infty}) \qquad (3\text{-}2)$$

Similar, a dimensionless wind-speed (WS) interference factor is

$$g \equiv (WS_\infty - WS)/WS_\infty \qquad (3\text{-}3)$$

and both quantities are bounded between 0 and 1.

Data for Ceramic modules were obtained on 2 occasions at the same location (Exps. 3b and 5a). The reduced data are listed in Tables IV and V. The test conditions(Table III) compare although buoyancy was a little stronger in Exp. 5a and the WS a little higher in Exp. 3b. The important thing to note in Tables IV and V is that the difference between (self) spray off and (self) spray on is appreciable and can not be neglected. As discussed earlier, the difference is attributed to self interference of the particular module tested. While the average values of $\bar{f}$ for (self) spray off are 0.20 and 0.29 for the two cases and this compares well with the previous recommended allowance of 0.22 [3],[4], the total interferences are much greater at 0.37 and 0.46, respectively. Self interference had been neglected from the point of view that NTU based on approach WBT was sufficient to describe performance of a single module. However, it is now clear that observed large self interference will not scale properly without account of $T-T_{WB_\infty}$ as incorporated in f.



RWP

The data for f (WBT) are plotted in Figure 5 for the case of (self) spray-on for both experiments as a function of row position. It should be noted that this f is the total operational interference allowance. The case of Exp. 3b is interesting in that the last two downwind rows exhibit some recovery back towards ambient WBT. Such phenomenon was also observed by Chen and Trezek [21] and was attributed to backside natural convection. However, in the present case, Exp. 3b has the lower buoyancy parameter and the greater wind speed which is not consistent with the argument. Instead it is possible that the difference is within experimental error.

The maximum error of the interference allowance based on accuracy of measured local wet-bulb temperature is estimated at ±15%, about the average scatter in the data. This percentage is based on f equal to a ratio of temperature differences, each temperature measured accurate to 0.1 C. The numerator is about 1-3 C (±7-20%) and the denominator 10-40 C (±0-2%) which adds to 7-22%. The bars with data points in Figure 5 represent the range of observed data. Also noted is a bar for ±15% error in the vicinity of the back-row decrease which could explain the behavior.

The nondimensional wind-speed interference factor g is plotted in Figure 6. In this case, there is substantially greater difference in the two experiments. The difference on the downwind side seems to be due to large fluctuations probably associated with large-scale atmospheric turbulence and unsteadiness after passing through and over the sprays. Whether this might affect performance to a like variation could be asked. However, the velocity of the spray ranges to order 10 m/s as discussed previously and so wind-speed changes of order 1 m/s or less should be of second-order importance. It indeed appears that the large local WS variations do not greatly affect f or, as shown later, NTU.

Data for the Richards modules (Figure 3) are shown in Table VI. Again, the difference between (self) spray off and (self) spray on is appreciable although the spray-off interference is somewhat less than that previously recommended [3,4]. Nevertheless, the total interference (spray on) is about 50% greater. Also shown in the table are data for essentially a single module ( S') wherein 11 neighboring modules were nonoperational as illustrated by nearly zero influence of other modules with spray off. The data show that Richards-module self interference dominates

over that of other surrounding modules. This may not be surprising in view of the spaces between Richards spray pattern (Figure 3). The f and g data are plotted versus row position in Figure 7 and 8, respectively, for the case of spray on.

NTU (ntu) Data

In this section, the experimental data are presented as reduced to NTU using the simplified analysis (NTU ≡ ntu). Data are reduced based on:

a) Canal measurements using assumed interference allowance (Exp. 1).
b) Module measurements using assumed interference allowance (Exp. 2).
c) Module measurements using measured interference allowance (Exp. 3-5).

Exp. 1-2 were performed at Dresden Station while the remainder were for Quad-Cities Station.

The NTU based on observed canal cooling performance of Ceramic modules at Dresden Station are plotted versus ambient wind speed in Figure 9. It is recalled that the canal segment has 2 rows across the canal and 20 passes along the canal for a total of 40 maximum operating modules. Quantity NTU were implied from canal temperatures at either end of the segment and therefore may be interpreted as "canal (averaged) NTU". An assumed average interference allowance of $\bar{f} = 0.10$ was used [3-4]. This allowance was predicated on f = 0 for the upwind row and f = 0.20 for the downwind row based a 40-ft (12.2-m) row spacing [5]. As discussed in the previous section, measured local WBT indicate somewhat higher interference in the first two rows of the 4-row Quad-Cities system. Data do not correlate very well with any single parameter. The lower-wind-speed data tend to indicate greater NTU with larger buoyancy parameter at the same 2.1-m bank height. However, the data for the greatest buoyancy parameter (0.09) may not have the greatest NTU because of the large bank height in this case. Insufficient data is available for independent correlation with all the parameters. As discussed later, the overall variation in NTU is not very great anyway.

For the purpose of an error analysis of the accuracy of ntu, for small ntu and $b_f/c_w \approx 1$, $\exp(-\text{ntu}\ b_f/c_w) \approx 1-\text{ntu}\ b_f/c_w$. It can be shown from Eqs. (2-7) and (2-12)



RWP

and the above that ntu for either a module or canal is approximately proportional to the ratio of cooling range to difference between canal temperature and WBT. Under typical conditions for either the present short canal or modules more generally, the numerator of the ratio is accurate to 0.2 C of 1-3 C (7-20%) while the denominator is accurate to 0.2 C of about 10-30 C (1-2%) which combines to an error from 8-22%. Thus, the average experimental accuracy for ntu is estimated within about ±15%. An error bar of ±15% is also shown in Figure 9, and the data show scatter not much greater than that.

The data of Figure 9 are substantially lower than that of [4] based on temperature data reported by Hoffman [24]. Present ntu range from 0.12 to 0.23 over 2.5-6.5 m/s. While previous ntu data ranged from 0.27 to 0.57 over 1-6.5 m/s [4]. However, the data base of Hoffman [24] was not fully documented, and module-NTU data discussed below tend to support the lower values found here.

Module NTU (ntu) also were determined at Dresden Station (Exp. 2). In this case, the spray was collected directly, and Eq.(2-7) yielded the value of NTU. The geometry is shown in Figure 1 and the NTU data in Table VII. As noted, Row I is always upwind as are "clock positions" 6 and 9. The experiment was performed in the center of a run of 8 continuous passes (16 modules). Data are selectively reduced for f = 0, 0.1 and 0.20. The first-row f was previously taken as 0, the second-row f as 0.20, and the average f as 0.10 [3-5]. As mentioned earlier, NTU is not expected to be greatly sensitive to f for a 2-row canal. We do not regard the reported distribution of NTU within the spray as being particularly significant in view of the use of a single WBT for a given spray. More significant is the spray-averaged NTU for each of the two rows. The module averaged NTU (ntu) were based on

$$\exp(-\text{ntu}\ b_f/c_w) = \sum_i \exp(-\text{ntu}_i\ b_f/c_w) \qquad (3\text{-}4)$$

which is equivalent to averaging the spray temperature except variation of WBT is accounted for.

The upwind row definitely tends to a greater NTU when the same f is employed. However, if sufficiently high f is used for the second row compared with the first, the two

NTU can be brought into agreement. Of the data shown, ntu = 0.116 with f = 0 for Row I is closest to ntu = 0.091 with f = 0.20 for Row II. These are the "previously recommended" local f values [5]. It is concluded that NTU is about the same for both rows but, of course, the local WBT is greater for Row II. As discussed in the previous section, there is considerable wind attenuation in spray systems as reflected in the g factor. However, NTU is apparently dominated by drop-wise factors due to the high trajectory velocity. Accordingly, wind attenuation would be expected to affect WBT (through f) more than affect NTU. Using f = 0.1, the pass-averaged ntu = 0.105 at 4.6 m/s (Exp. 2) is compatible with the lower range of canal-averaged ntu (Exp. 1) as shown in Figure 9.

Module NTU were also obtained for Ceramic modules at Quad-Cities Station (Exps. 3a and 5b) as illustrated in Figure 2. Data are listed in Tables VIII and IX. The experimental f is based on having the individual module "spray on" which includes self interference. As in the case of Dresden Station, the present data (Tables VIII and IX) show a trend toward greater NTU on the windward side of an individual spray although the use of a single WBT for an individual spray probably precludes qunatitative resolution of NTU within a spray. The spray-averaged data are plotted in Figure 10. The vertical bars denote ranges of observed data while the symbols are at the average values.

In the case of Exp. 5b (Table IX), it was noted during the experiment that the cone-impact supports of the spray nozzles were producing somewhat abnormal spray patterns over 0.5m of the perimeter at the usually selected 3-6-9-12 O'clock positions. Therefore, alternate positions shifted 45$^{o}$ (1:30-4:30-7:30-10:30) were selected. The abnormal pattern may be due to algae growth, but did not appreciably alter the overall pattern. It is interesting to note that the phenomenon was not observed in the earlier experiment (Table VIII) and that data appear consistant considering the difference in wind speed and experimental accuracy. It is uncertain whether the true integrated module NTU would be greater (due to WBT venting) or less (due to drop coalescence) than that of the normal spray pattern. All that can be said is that the abnormality is localized and because the physical extent is only a total of about 2m of the 40m perimeter, the integrated NTU is likely not altered more than about 5%.



RWP

As noted in the tables, some experimental f values used in data reduction were actually obtained from data taken at a different time. However, the local WBT used in reducing NTU was based on the actual prevailing ambient WBT and canal temperature. Some cases where both instantaneous and other f values were used are shown in Table IX. The NTU agree with the ±15% error estimate which supports the approach. Also noted in Table VIII are some single row ("S") data taken by turning off the 3 other rows for 3 passes (150 m), and data were taken in the center of the run. The average module NTU is 0.144 for the single row which compares with the pass-averaged value of 0.136 for 4 rows well within ±15%.

Once again, the evidence points toward NTU being primarily dominated by drop-wise phenomena and independent of conditions when local WBT is employed. The above module NTU data are plotted versus wind speed in Figure 11. In one case (Exp. 5b), data are plotted using both ambient and local wind speed, the effect being inconclusive. While there is a trend toward greater module NTU at greater wind speed, as was the case for canal NTU in Figure 9, the effect is not large. Indeed, based on local WBT

$$\text{ntu (Ceramic)} = 0.15 \pm 15\% \qquad (3\text{-}5)$$

$$1 \leq WS \leq 6 \text{ m/s}$$

fits 67% of the 33 data of both Figure 9 and Figure 11. All but one of the data (97%) are bounded by ntu = 0.15 ±33% over the WS interval 1-6 m/s.

Data were also taken for the Richards of Rockford modules at Quad-Cities (Exp. 4a) with the geometry of Figure 3. Data are listed in Table X and were based on simultaneous local WBT measurements. Unfortunately, mooring cables prevented convenient traversing of the Richards spray. Time was available only for a few samples as noted. Fortunately, these included a single module case (3 passes otherwise turned off, an interval of 120 m) and a Pow IV (most downwind) case which probably bound the possible range of NTU for prevailing conditons. Using the experimental f, ntu module-averaged are 0.058 and 0.066 respectively which together average to 0.062 ±6%, well within the ±15% estimated error. We conclude, based on local WBT



RWP

ntu (Richards) $\approx$ 0.06

WS $\approx$ 2 m/s (3-6)

but must caution against any confidence in using such a value owing to the extremely limited data base. Further, caution must be made against a comparison of Eq. (3-5) and Eq. (3-6), without further considerations. The flow rates of the two modules differ for Ceramic and Richards (10,000 gpm and 12,000 gpm-nominal, repectively) as likely do cost and possibly numerous other factors such as pump power, maintenance, reliability, etc.

## SUMMARY OF CONCLUSIONS

Equations for unit (spray or spray module) and systems (spray canal) cooling were derived from fundamental consideration of heat and mass transfer wherein the principal unknown drop parameters are combined into NTU. A dimensionless interference allowance f was introduced to incorporate local heating and humidification effects.

While the present data base is limited, it appears as though NTU for a particular spray module is relatively constant and independent of conditions so long as a local wet-bulb temperature is employed in the equations, such as that 2m over the water surface at the center of the module in plan. The dimensionless interference allowance relates the local increment of wet-bulb temperature above ambient to the local liquid water and ambient wet-bulb temperatures. The present experimental values as a function of position windward through the spray field may be useful for estimating performance under similar conditions and for developing fluid dynamic models of the effect.

## REFERENCES

1. Yang, U.M. and Porter, R.W., "Thermal Performance of Spray Cooling Systems-Theoretical and Experimental Aspects", IIT Waste Energy Management Report TR-76-1, December 1976.

2. Chaturvedi, S. and Porter, R.W., "Air-Vapor Dynamics in Large-Scale Atmospheric Spray Cooling Systems", IIT Waste Energy Management Report TR-77-1, March 1977.



RWP

3. Porter, R.W., Yang, U.M. and Yanik, A., "Thermal Performance of Spray Cooling Systems", Proceedings of American Power Conference, Vol. 38, 1976, p. 1458-1472.

4. Porter, R.W., "Analytical Solution for Spray-Canal Heat and Mass Transfer", Joint ASME Paper 74-HT-58, AIAA Paper 74-764, July 1974.

5. Porter, R.W. and Chen, K.H., "Heat and Mass Transfer of Spray Canals", Journal of Heat Transfer, Vol. 96,3 August 1974, p. 286.

6. Frohwerk, P.A., "Spray Modules Cool Plant Discharge Water", Power, Vol. 115, September 1971, p. 52-53.

7. Kelley, R.B., "Large Scale Water Cooling Via Floating Spray Devices', Energy Production and Thermal Effects Ann Arbor Science Publishers, January 1974, p. 92.

8. Sherwood, T.K., Pigford, R.L., and Wilke, C.R., Mass Transfer, McGraw-Hill, NY, 1975, p. 26.

9. Threlkeld, J.L., Thermal Environmental Engineering, Prentice Hall, Englewood Cliffs, Part III, 1970.

10. Levich, V.G., Physicochemical Hydrodynamics, Prentice Hall, Englewood Cliffs, 1962.

11. Gunn, R. and Kinzer, G.D., "The Terminal Velocity of Fall for Water Droplets in Stagnant Air", Journal of Meteorology, Vol. 6, August 1949, p. 243-248.

12. Chao, B.T., "Transient Heat and Mass Transfer to a Translating Droplet", Journal of Heat Transfer, Vol. 91, No. 2, May 1969, p. 273.

13. Mori, Y. et al., "Unsteady Heat and Mass Transfer from Spheres", International Journal of Heat and Mass Transfer, Vol. 12, 1969, p. 571.

14. Ranz, W.E. and Marshall, W.R. Jr., "Evaporation From Drops", Chemical Engineering Progress, Vol. 48, 1952, p. 141-146, 173-180.

15. Yao, S.C. and Schrock, V.E., "Heat and Mass Transfer from Freely Falling Drops", Journal of Heat Transfer, Vol. 98, February 1976, p. 120-126.

16. Hebden, W.E. and Shah, A.M., "Effects of Nozzle Performance on Spray Ponds", Proceedings of American Power Conference, Vol. 38, 1976, p. 1449-1457.

17. Chen, K., Heat and Mass Transfer from Power Plant Spray Cooling Ponds", Ph.D Dissertation, University of California, Berkeley, May 1975.

18. Hollands, K.G.T. and Goel, K.C., "Mean Diameters in Parallel-Flow and Conter-Flow Aerosol Systems", Journal of Heat Transfer, Vol. 98, May 1976, p. 297-302.

19. Elgawhary, A.M. and Rowe, A.M., "Spray Pond Mathematical Model for Cooling Fresh Water and Brine', Environmental and Geophysical Heat Transfer, ASME HT-Vol. 4, 1971.

20. Ryan, P.J. and Myers, D.M., "Spray Cooling A Review of Thermal Performance Models", Proceedings of American Power Conference, Vol. 38, 1976, p. 1473-1461.

21. Chen, K.H. and Trezek, G.J., "Spray Energy Release (SER) Approach to Analyzing Spray System Performance", Proceedings of American Power Conference, Vol 38, 1976, p. 1435-1448.

22. Schlichting, H., Boundary Layer Theory, 6th Edition, McGraw-Hill, New York, 1968.

23. Kelley, R.B., "Large-Scale Spray Cooling", Industrial Water Engineering, Vol. 8 August-September 1971, p. 18-20.

24. Hoffman, D.P., "Spray Cooling for Power Plants", Proceedings of American Power Conference, Vol. 35, 1973, p. 702.

25. Soo, S.L., "System Considerations in Spray Cooling and Evaporation", Proceedings of American Power Conference, Vol. 38, 1976, p. 1482-1486.

26. Soo, S.L., "Power Spray Cooling-Unit and System Performance", ASME Paper 75-WA/Pwr-3, December 1975.

27. Arndt, C.R. and Barry, R.E., "Simulation of Spray Canal Cooling for Power Plants-Performance and Environmental Effects", ASME Paper 76-WA/HT-28, December 1976.

28. Bird, R., Stewart, W.E. and Lightfoot, E.N., Transport Phenomena, Wiley, NY, 1960, p. 495.

29. Berry, C.H., "Mixtures of Gases and Vapors", Mechanical Engineer's Handbook, Edited by T. Baumeister, McGraw-Hill, NY, 1958, p. 4-82.

30. Frass, A.P. and Ozisik, M.M., Heat Exchanger Design, Wiley, NY, 1965, Chapter 15.

TABLE I. SPRAY MODULE PARAMETERS

| | Ceramic Cooling Tower (CCT) Co. | Richards of Rockford (RR) |
|---|---|---|
| Flow Rate ($\ell$/min) | $3.8 \times 10^4$ | $4.5 \times 10^4$ |
| Sprays/Module | 4 | 1 |
| Pump Motor Power (Kw) | 51 | 56 |
| Spray Diameter (m) | 12.2 | 16.0 |
| Spray Height (m) | 5.5 | 5.2 |

TABLE II. TABULATION OF $b(T)/c_w = h'(T)/c_w$.

| T(C) → | 0 | 10 | 20 | 30 | 40 |
|---|---|---|---|---|---|
| 0 | 0.395 | 0.545 | 0.785 | 1.185 | 1.845 |
| 1 | 0.410 | 0.563 | 0.816 | 1.239 | 1.930 |
| 2 | 0.415 | 0.584 | 0.850 | 1.293 | 2.030 |
| 3 | 0.425 | 0.606 | 0.888 | 1.347 | 2.125 |
| 4 | 0.430 | 0.627 | 0.924 | 1.407 | 2.238 |
| 5 | 0.445 | 0.650 | 0.960 | 1.470 | 2.345 |
| 6 | 0.485 | 0.677 | 1.001 | 1.537 | 2.465 |
| 7 | 0.500 | 0.700 | 1.045 | 1.609 | 2.590 |
| 8 | 0.510 | 0.726 | 1.090 | 1.660 | 2.720 |
| 9 | 0.530 | 0.754 | 1.135 | 1.755 | 2.870 |

TABLE III. SUMMARY OF FIELD EXPERIMENTS("D" DENOTES DRESDEN STATION AND "Q" QUAD-CITIES STATION).

| Exp. | Date | Station and Module | Object | $T_f$ (C) | WS (m/s) | WD (°) | $\frac{\lvert\Delta\rho\rvert}{\rho}$ | $z_B$ (m) |
|---|---|---|---|---|---|---|---|---|
| 1 | 3-17-75 | D,CCT | (canal ntu) | 11 | 3.0 | 84-89 | .09 | 2.4 |
| | 3-18-75 | " | " | 18 | 5.0-6.4 | 51-74 | .03 | 2.3 |
| | 8-20-75 | " | " | 32 | 2.5-3.0 | 7-90 | .06 | 2.1 |
| | 8-21-75 | " | " | 32 | 2.6-3.5 | 71-86 | .05 | 2.1 |
| 2 | 6-16-76 | " | (module ntu) | 24 | 4.6 | 10 | .065 | 2.4 |
| 3a | 6-30-76 | Q,CCT | (module ntu) | 23 | 4.6 | 19 | .043 | 2.0 |
| 3b | 7-1-76 | " | f | 24 | 2 | 52 | .035 | 2.0 |
| 4a | 7-27-76 | Q,RR | (module ntu& f) | 29 | 2.2 | 97 | .045 | 1.2 |
| 4b | 7-29-76 | " | f | 29 | 2.1 | 118 | .078 | 2.7 |
| 5a | 9-28-76 | Q,CCT | f | 20 | 1.3 | 30 | .043 | 2.0 |
| | 9-29-76 | " | " | 20 | 1.8 | 61 | .041 | 2.0 |
| 5b | 9-29-76 | " | (module ntu& f) | 20 | 2.4 | 81 | .038 | 2.0 |

TABLE IV. INTERFERENCE ALLOWANCE OF EXP. 3b, CERAMIC MODULES (ROW I IS UPWIND).

| $Row_1$ | $f_1$ | | $g_1$ | |
|---|---|---|---|---|
| | Spray Off | Spray On | Spray Off | Spray On |
| I | 0.20 | 0.20 | 0.27 | 0.39 |
| " | 0.06 | 0.23 | 0.13 | 0.40 |
| I(avg.) | 0.13 | 0.21 | 0.20 | 0.40 |
| II | 0.28 | 0.49 | 0.35 | 0.50 |
| " | 0.27 | 0.47 | 0.29 | 0.54 |
| II(avg.) | 0.27 | 0.48 | 0.32 | 0.52 |
| III | 0.25 | 0.38 | 0.28 | 0.37 |
| " | 0.31 | 0.46 | 0.32 | 0.50 |
| III(avg.) | 0.28 | 0.42 | 0.30 | 0.44 |
| IV | 0.15 | 0.40 | 0.46 | 0.08 |
| " | 0.11 | 0.38 | 0.25 | 0.40 |
| IV(avg.) | 0.13 | 0.39 | 0.36 | 0.24 |
| Overall Avg. | 0.20 | 0.37 | 0.30 | 0.40 |

TABLE V. INTERFERENCE ALLOWANCE OF EXP. 5a, CERAMIC MODULES (ROW I IS UPWIND)

| | $f_i$ | | $g_i$ | |
|---|---|---|---|---|
| $Row_i$ | Spray Off | Spray On | Spray Off | Spray On |
| 9-28-76 | | | | |
| I | 0.164 | 0.096 | 0.03 | 0.21 |
| " | 0.029 | 0.317 | 0.28 | 0.18 |
| I(avg.) | 0.097 | 0.207 | 0.15 | 0.20 |
| II | 0.270 | 0.454 | 0.09 | 0.05 |
| " | 0.323 | 0.338 | - | 0.02 |
| II(avg.) | 0.297 | 0.396 | 0.09 | 0.03 |
| 9-29-76 | | | | |
| I | 0.191 | 0.228 | 0.34 | 0.04 |
| " | 0.168 | 0.374 | 0.30 | 0.09 |
| I(avg.) | 0.180 | 0.301 | 0.32 | 0.07 |
| II | 0.284 | 0.409 | 0.07 | 0.08 |
| " | 0.200 | 0.307 | 0.21 | 0.30 |
| II(avg.) | 0.242 | 0.358 | 0.14 | 0.19 |
| III | 0.278 | 0.425 | 0.32 | 0.30 |
| " | 0.310 | 0.437 | 0.37 | - |
| III(avg.) | 0.294 | 0.431 | 0.35 | 0.30 |
| IV | 0.429 | 0.563 | 0.26 | 0.47 |
| " | 0.429 | 0.486 | 0.45 | 0.32 |
| IV(avg.) | 0.429 | 0.524 | 0.36 | 0.40 |
| Overall Avg. | 0.29 | 0.46 | 0.29 | 0.24 |

TABLE VI. INTERFERENCE ALLOWANCE OF EXP. 4a AND 4b, RICHARDS MODULES (ROW I IS UPWIND, "S" IS FOR SINGLE MODULE)

| Row$_i$ | $f_i$ | | $g_i$ | |
|---|---|---|---|---|
| | Spray Off | Spray On | Spray Off | Spray On |
| Exp. 4a | | | | |
| IV | - | 0.390 | - | 0.38 |
| " | - | 0.391 | - | 0.45 |
| " | - | 0.384 | - | 0.36 |
| " | - | 0.341 | - | 0.32 |
| IV(avg.) | - | 0.376 | - | 0.38 |
| S | - | 0.158 | - | 0.42 |
| " | - | 0.161 | - | 0.42 |
| " | - | 0.149 | - | 0.38 |
| S(avg.) | - | 0.156 | - | 0.41 |
| Exp. 4b | | | | |
| I | 0.056 | 0.031 | 0.22 | 0.33 |
| II | 0.111 | 0.218 | 0.05 | 0.26 |
| " | 0.186 | 0.420 | 0.05 | - |
| II(avg.) | 0.149 | 0.319 | 0.05 | 0.26 |
| III | 0.172 | 0.315 | - | - |
| " | 0.243 | 0.303 | - | - |
| III(avg.) | 0.208 | 0.309 | - | - |
| IV | 0.174 | 0.323 | - | - |
| Overall Avg. | 0.15 | 0.25 | - | - |
| S | 0.007 | 0.314 | - | - |
| " | 0.014 | 0.234 | - | - |
| S(avg.) | 0.011 | 0.274 | - | - |

TABLE VII. MODULE NTU(ntu) OF EXP. 2 BASED ON RECOMMENDED INTERFERENCE $\bar{f}$ [3,4], CERAMIC MODULES, DRESDEN STATION ("CLOCK POSITION" 6 AND 9 ARE ALWAYS UPWIND).

| | ntu(based on:) | | |
|---|---|---|---|
| Row i | f = 0 | $\bar{f}$ = 0.1 | f = 0.2 |
| I- 6 | 0.086 | 0.096 | |
| I- 3 | 0.086 | 0.096 | |
| I-12 | 0.138 | 0.154 | |
| I- 9 | 0.157 | 0.176 | |
| I(avg.) | 0.116 | 0.130 | |
| II- 6 | | 0.072 | 0.082 |
| II- 3 | | 0.117 | 0.133 |
| II- 3 | | 0.080 | 0.089 |
| II-12 | | 0.080 | 0.089 |
| II- 9 | | 0.054 | 0.061 |
| II(avg.) | | 0.080 | 0.091 |
| Overall | | 0.105 | |

TABLE VIII. MODULE NTU (ntu) OF EXP. 3a, CERAMIC MODULES, BASED ON EXPERIMENTAL f WITH SPRAY ON FROM EXP. 3b.

| Row i | ntu |
|---|---|
| I - 6 | 0.132 |
| 3 | 0.097 |
| 12 | 0.124 |
| 9 | 0.156 |
| I(avg.) | 0.127 |
| II- 6 | 0.136 |
| 3 | 0.217 |
| 12 | 0.169 |
| 9 | 0.260 |
| II(avg.) | 0.196 |
| III-6 | 0.146 |
| 3 | 0.147 |
| 12 | 0.145 |
| 9 | 0.141 |
| III(avg.) | 0.145 |
| IV- 6 | 0.162 |
| 3 | 0.112 |
| 12 | 0.149 |
| 9 | 0.240 |
| IV(avg.) | 0.166 |
| Overall(avg.) | 0.158 |

TABLE IX MODULE NTU(ntu) OF EXP. 5b, CERAMIC MODULES, BASED ON EXPERIMENTAL f WITH SPRAY ON.

| Row i | ntu (based on:) f(5a) | f(5b) |
|---|---|---|
| I- 7:30 | 0.132 | - |
| 4:30 | 0.139 | - |
| 1:30 | 0.145 | - |
| 10:30 | 0.095 | - |
| I(avg.) | 0.128 | - |
| II- 4:30 | 0.178 | - |
| 7:30 | 0.229 | - |
| 10:30 | 0.105 | - |
| 1:30 | 0.120 | - |
| II(avg.) | 0.158 | - |
| III- 4:30 | 0.133 | - |
| 7:30 | 0.152 | - |
| 10:30 | 0.099 | - |
| 1:30 | 0.117 | - |
| III(avg.) | 0.125 | - |
| IV- 4:30 | 0.139 | 0.126 |
| 7:30 | 0.140 | - |
| 10:30 | 0.141 | - |
| 1:30 | 0.120 | 0.126 |
| IV(avg.) | 0.135 | - |
| Overall (avg.) | 0.136 | - |
| S- 4:30 | - | 0.170 |
| 1:30 | - | 0.118 |
| S(avg.) | - | 0.144 |

TABLE X. MODULE NTU(ntu) OF EXP. 4a, RICHARDS MODULES EXPERIMENTAL f.

| Row i | f Experimental | ntu (Exp. f) |
|---|---|---|
| IV- 9 | 0.390 | 0.074 |
| 6 | 0.391 | 0.068 |
| 12 | 0.384 | 0.084 |
| 3 | 0.340 | 0.039 |
| IV(avg.) | 0.376 | 0.066 |
| S- 3 | 0.158 | 0.046 |
| 6 | 0.161 | 0.074 |
| 12 | 0.149 | 0.053 |
| S(avg.) | 0.156 | 0.058 |

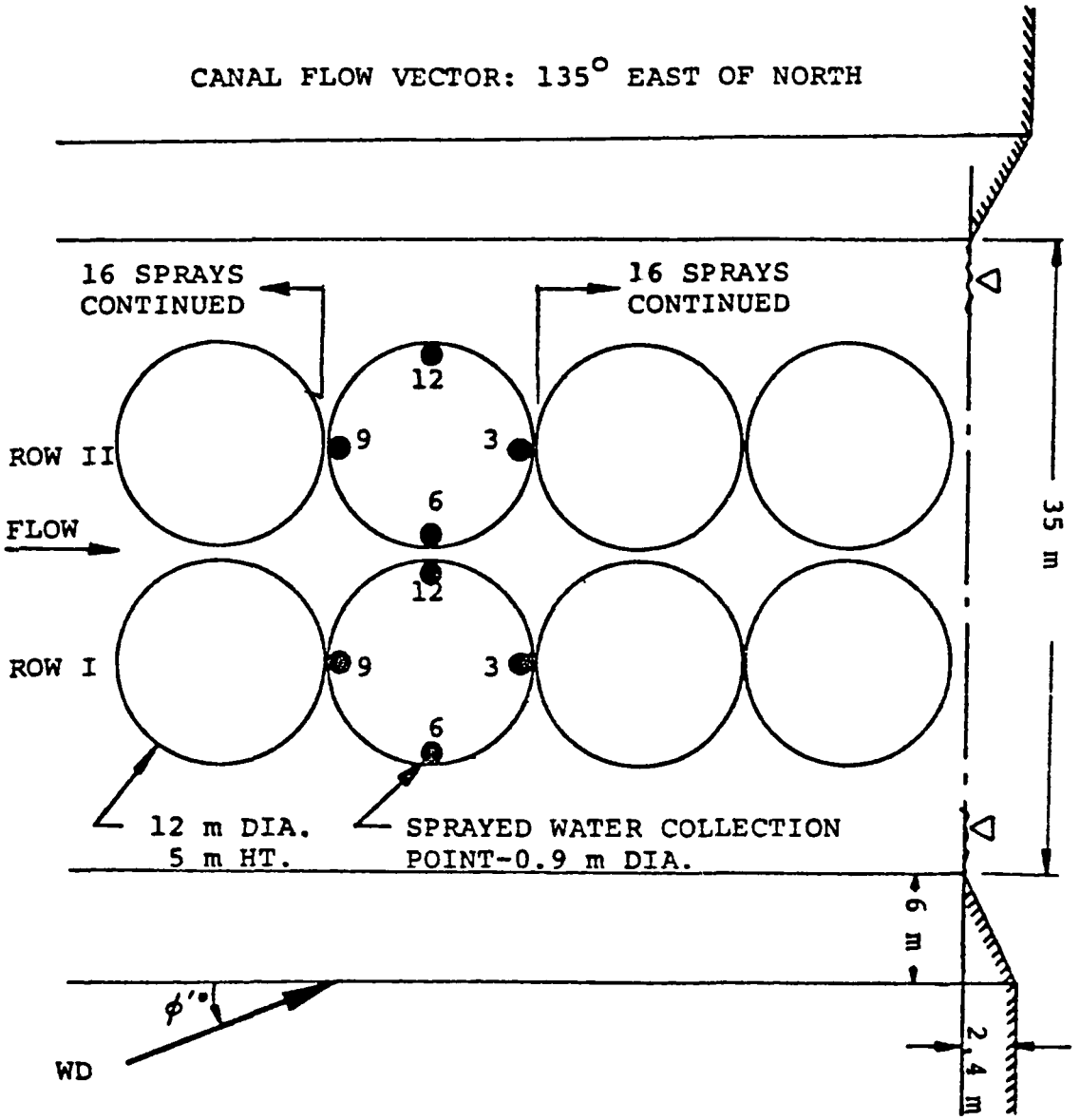


Figure 1 . Geometry of Ceramic Modules at Dresden Station (Experiment 2).

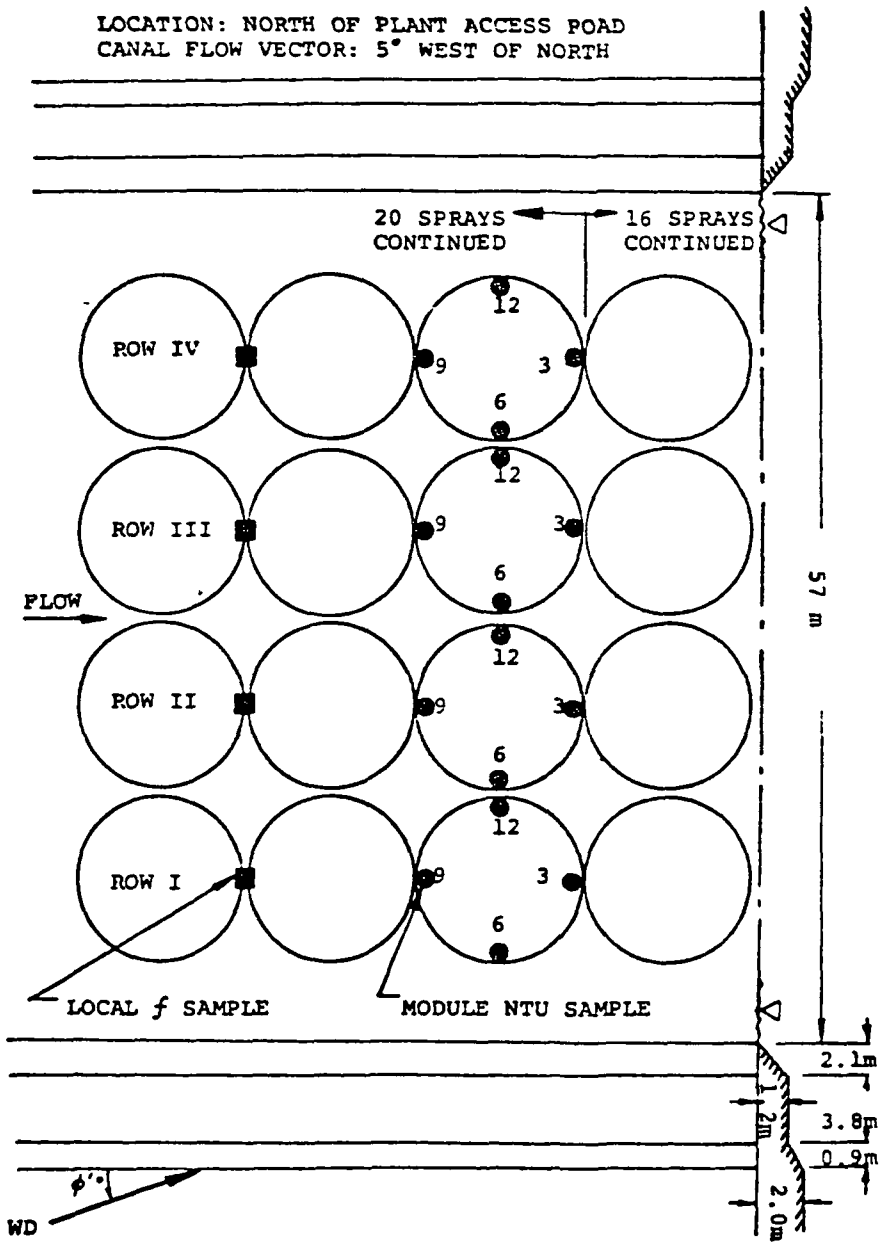


Figure 2. Geometry of Ceramic Modules at Quad-Cities Station (Experiment 3).

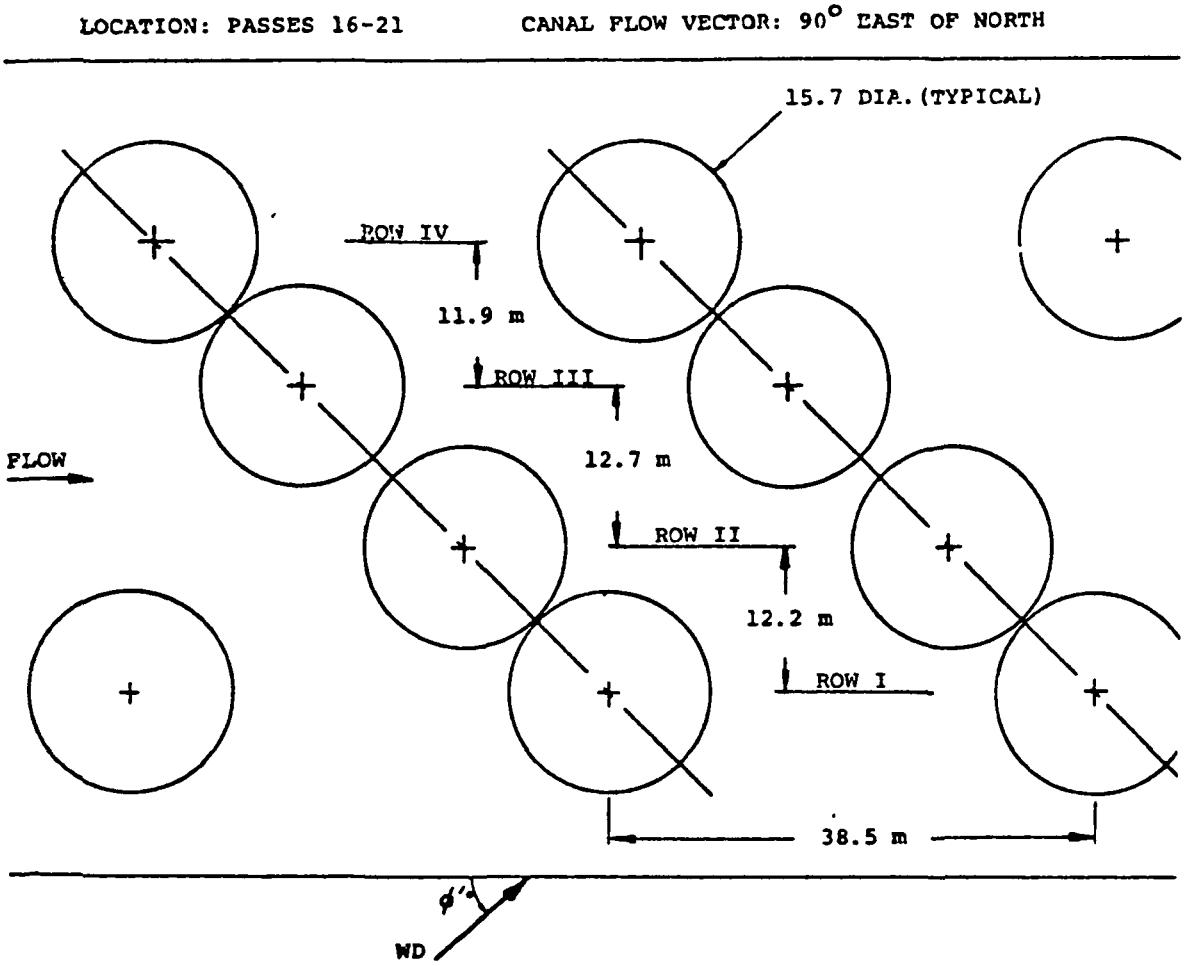


Figure 3. Geometry of Richards Modules at Quad-Cities Station (Experiment 4).

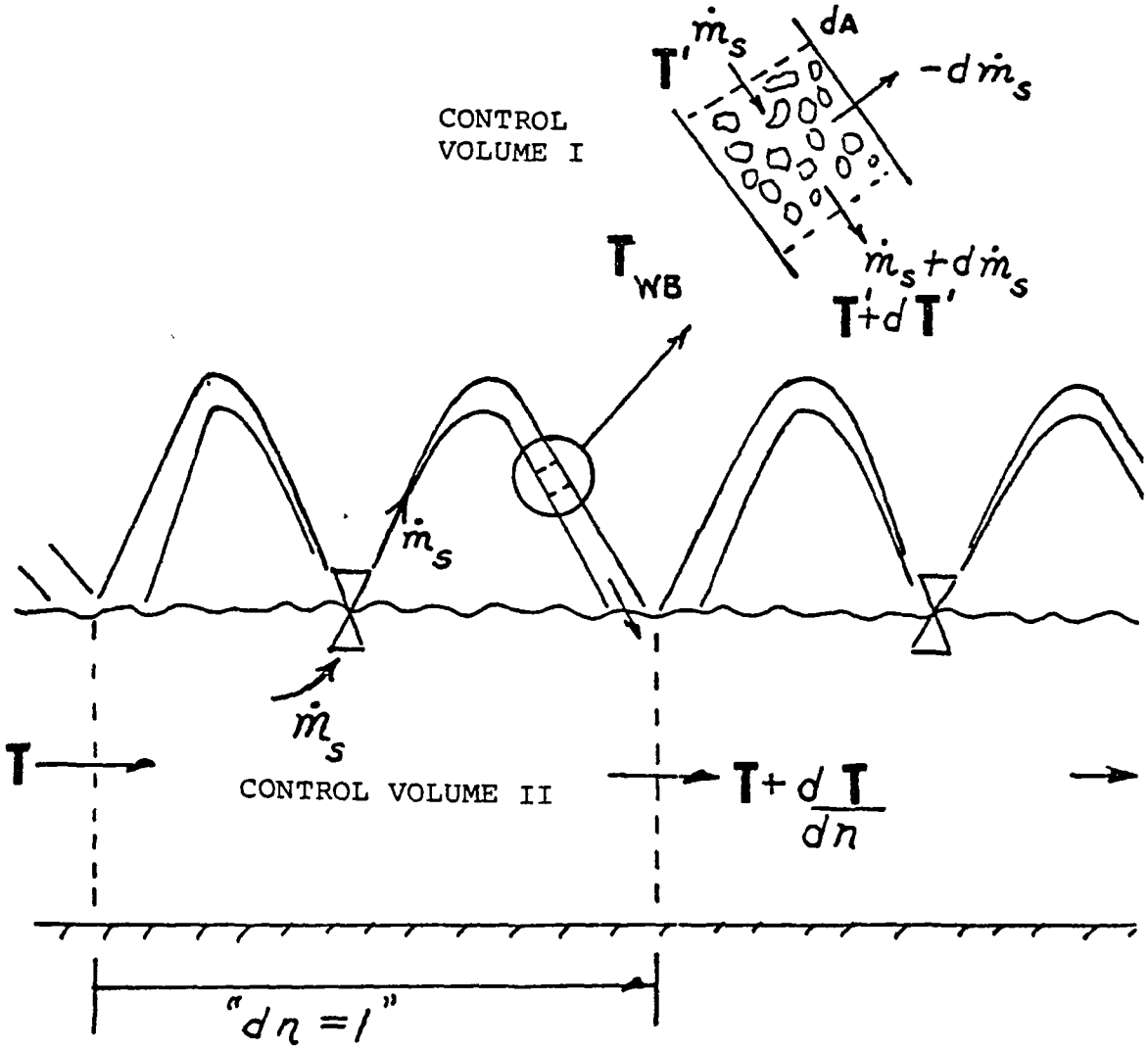


Figure 4. Control Volumes for Spray (I) and Canal (II).

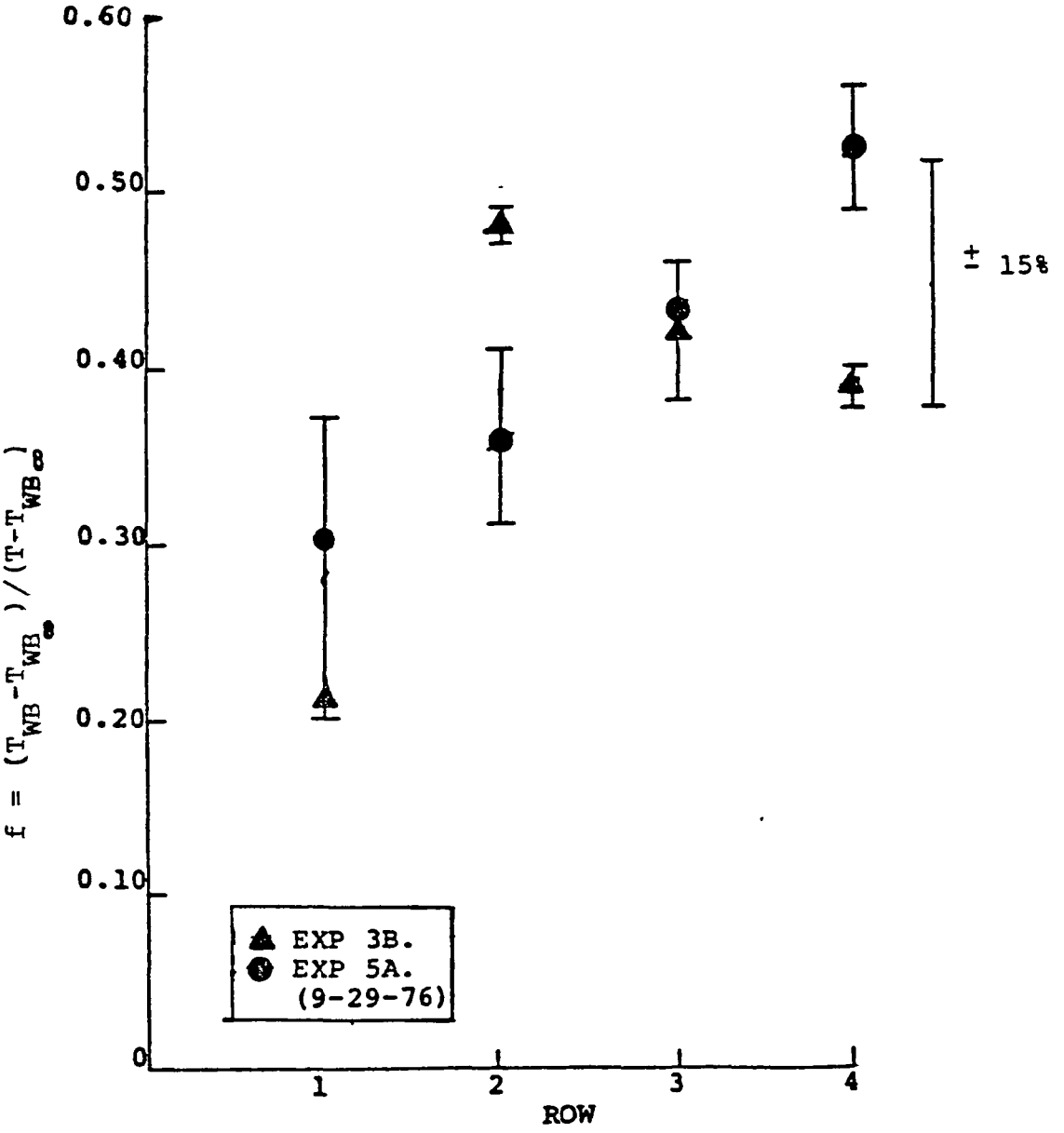


Figure 5. Local WBT Interference Allowance (Spray On) for Ceramic Modules at Quad-Cities Station.

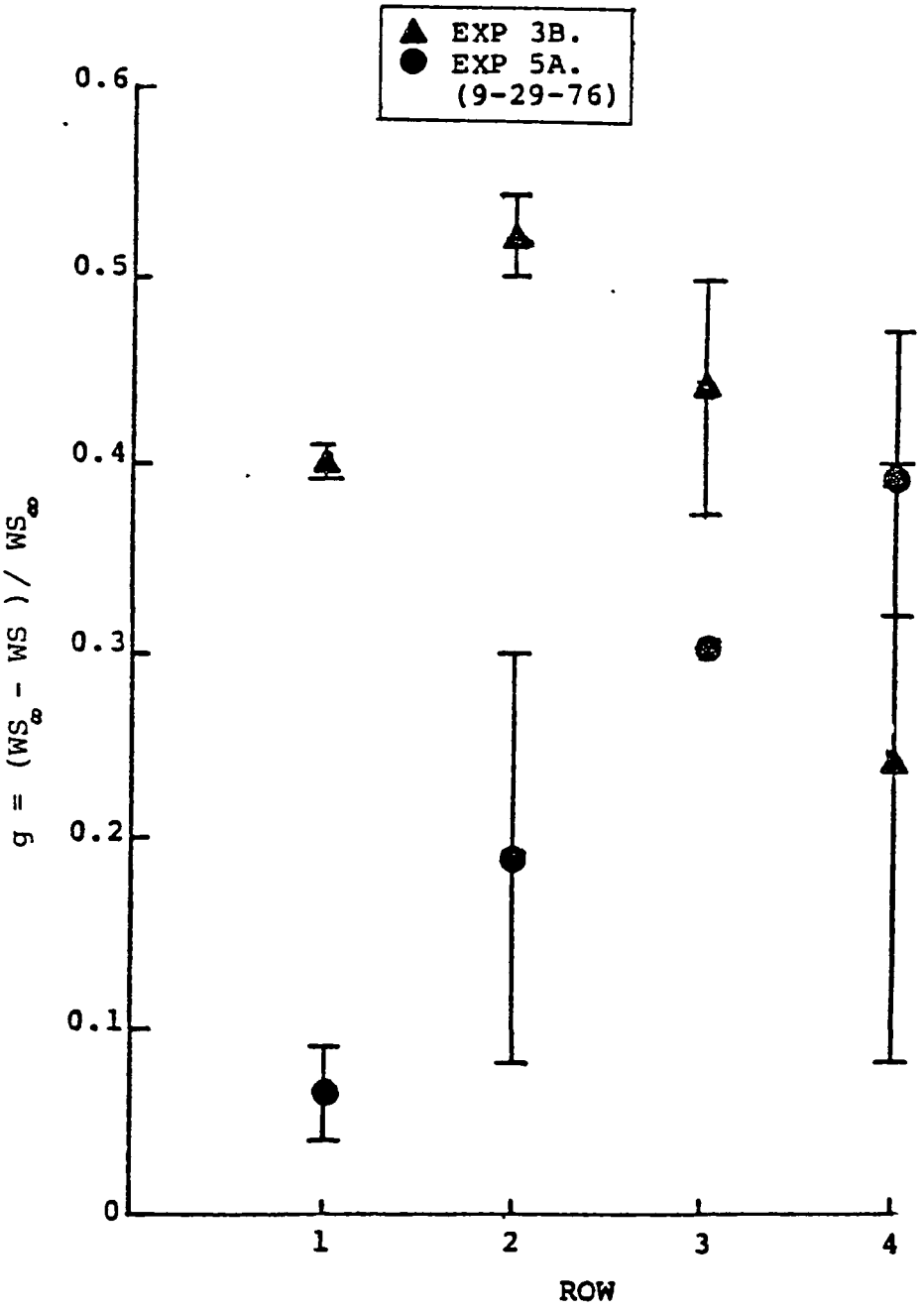


Figure 6. Local Wind Speed Increment Ratio versus Row Position for Ceramic Module.

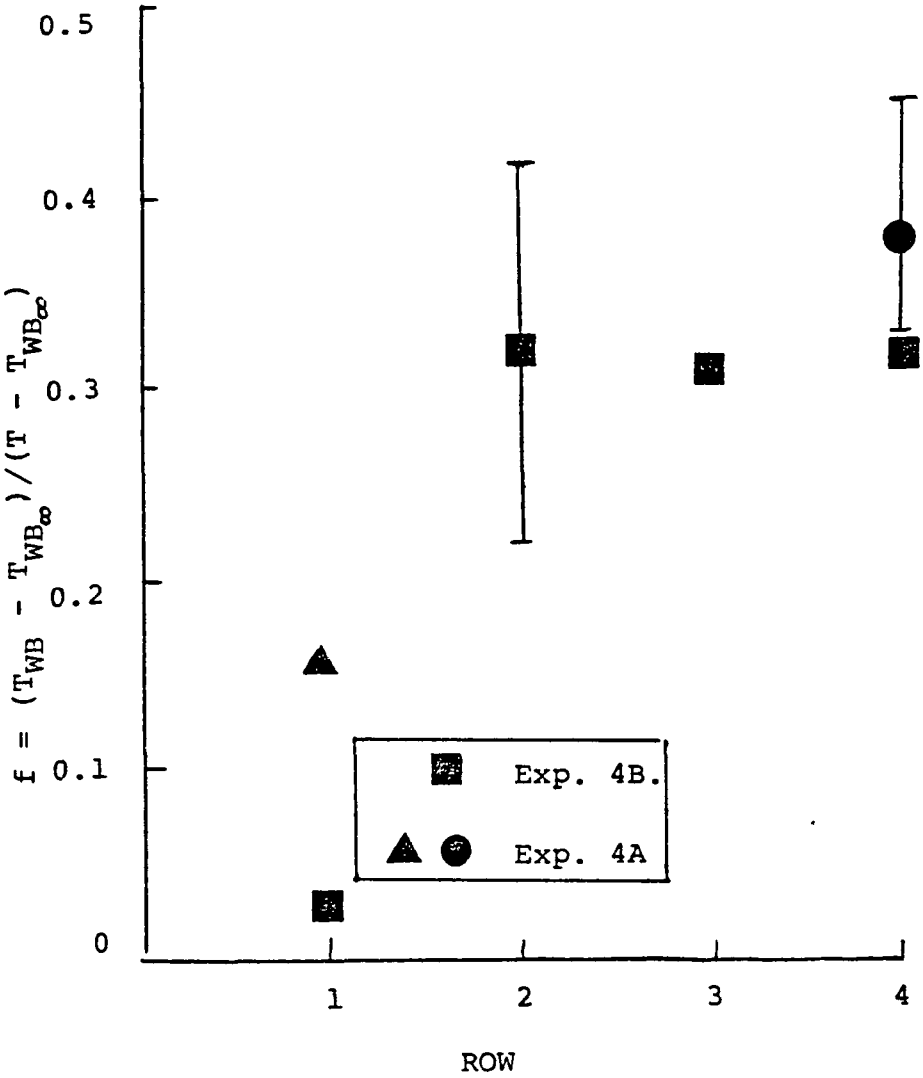


Figure 7. Local WBT Interference Allowance(Spray On) for Richards Modules at Quad-Cities Station.

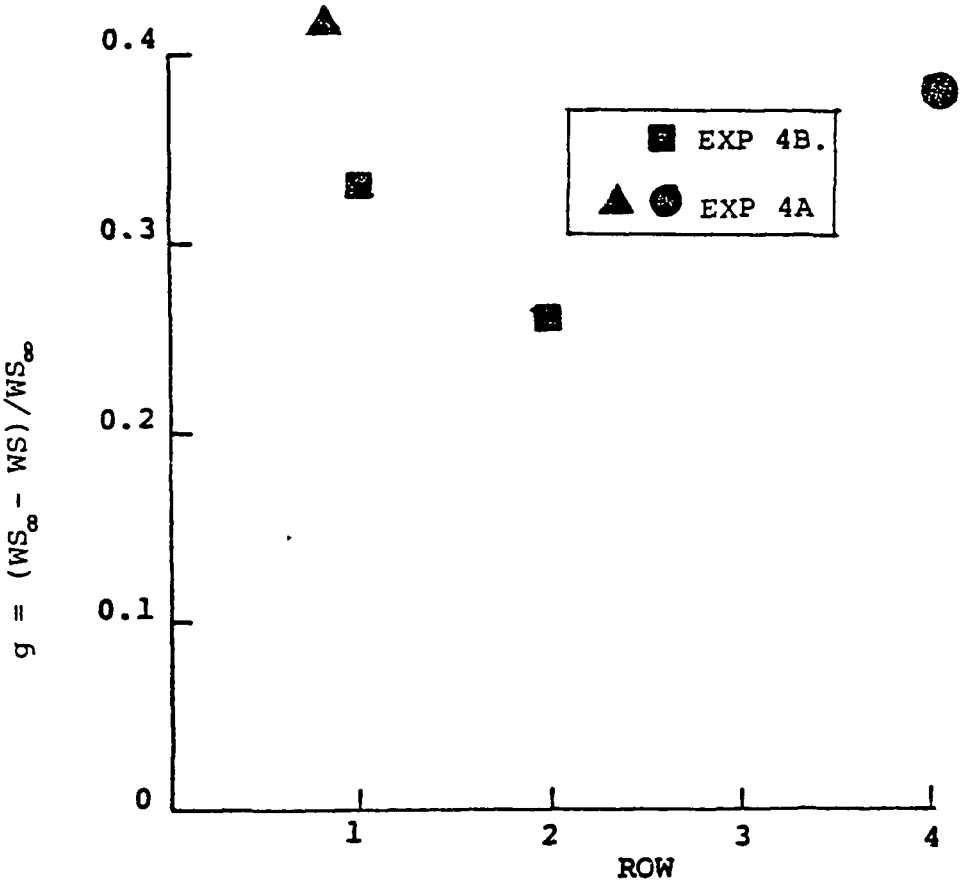


Figure 8. Local Wind Speed Increment Ratio (Spray On) versus Row Position for Richards Module at Quad-Cities Station.

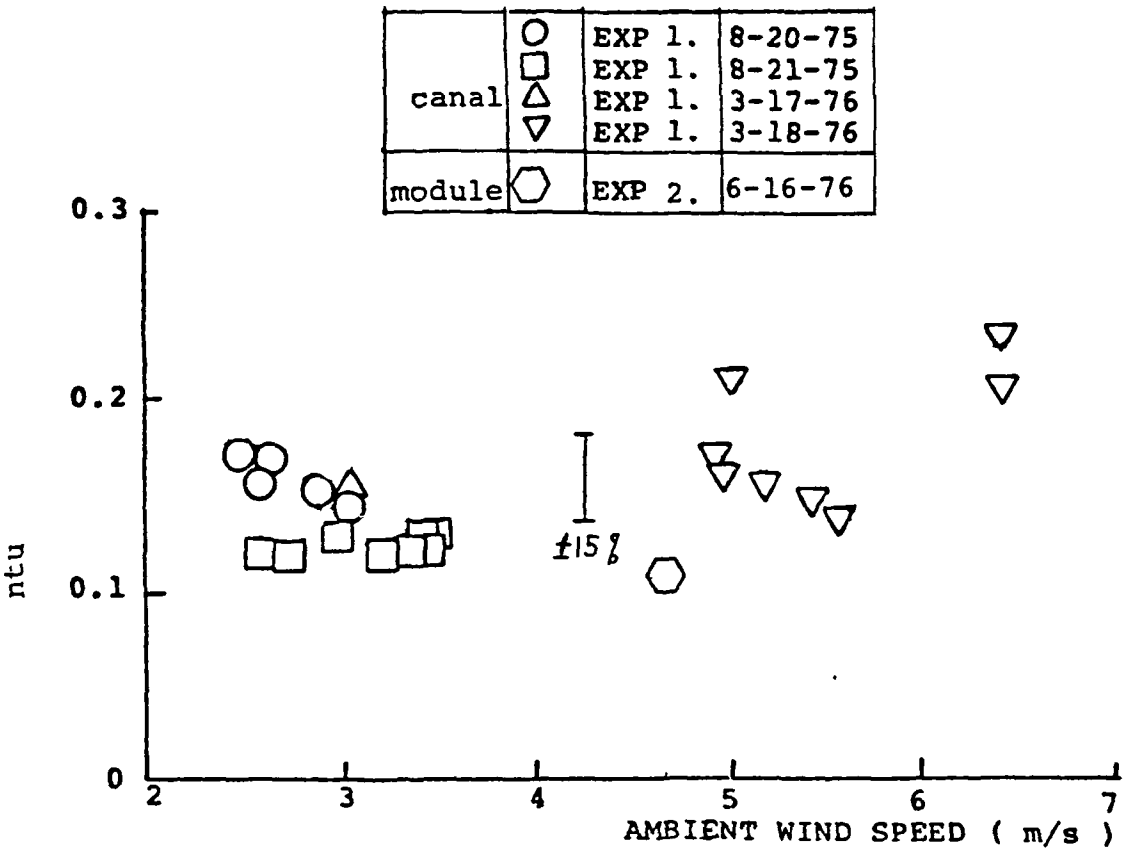


Figure 9. Canal and Module ntu Based on Interference Allowance of 0.1 for 2-Row Ceramic Modules at Dresden Station .

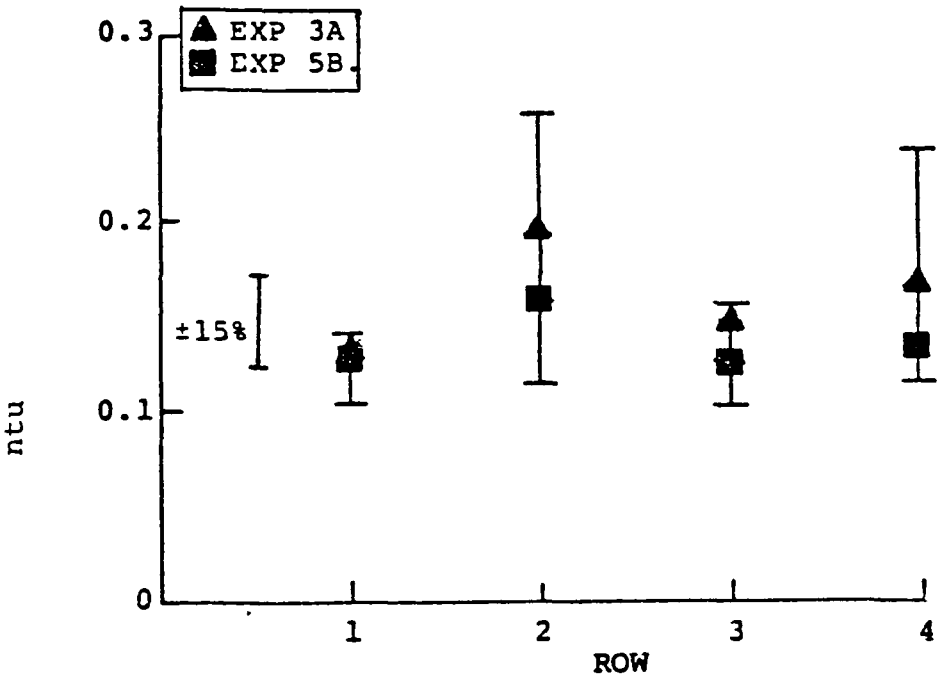


Figure 10. Module ntu Based on Exp.f, Ceramic Modules at Quad-Cities Station.

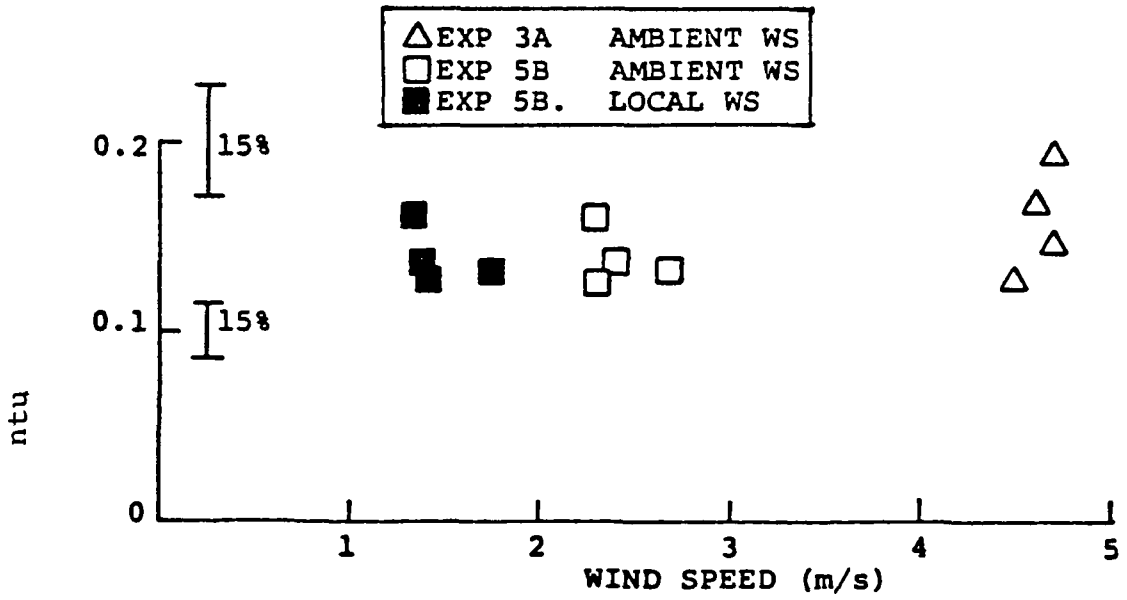


Figure 11. Module ntu Based on Experimental f, Ceramic Modules, Quad-Cities Station.